Infrared Active Methyl Group Vibrations in Tetratetracontane: A Probe for Chain End Organization and Crystal Structure

Jean-Philippe Gorce,[†,‡] Stephen. J. Spells,[*,†] Xiang-Bing Zeng,[§] and Goran Ungar[§]

Materials Research Institute, Sheffield Hallam University, City Campus, Sheffield S1 1WB, United Kingdom, and Department of Engineering Materials, University of Sheffield, Sheffield S1 3JD, United Kingdom

Received: June 26, 2003; In Final Form: October 28, 2003

By crystallizing tetratetracontane (n-$C_{44}H_{90}$) from solution in toluene under a variety of conditions, the orthorhombic I and (011) tilted monoclinic forms were identified by X-ray diffraction (XRD) and the orthorhombic II form was inferred from infrared spectroscopy. Application of pressure to the crystal mat resulted in a proportion of triclinic structure. At 75 °C, the (011) monoclinic form transforms to a (101) tilted monoclinic phase. Differing extents of chain end and translational disorder are believed to be responsible for these different crystal forms, which were studied using the conformational sensitivity of several infrared-active methyl and methylene group vibrations. Depending on the crystal phase, the symmetric methyl deformation around 1378 cm^{-1} shows differing characteristics, and both the rocking and the asymmetric C−H stretching vibrations show different components. An increase in the end-*gauche* methylene wagging absorbance in the (101) monoclinic structure with increasing temperature together with the presence of even order bands from the CH_2 methylene rocking−twisting progression are also attributed to chain end disorder. The implications of the results on the methyl symmetric deformation for the use of the methylene wagging region of the spectrum to characterize disorder in alkyl chains are discussed.

Introduction

Short chain *n*-alkanes crystallize from solution in the form of thin lozenges and show a diversity of crystal structures.[1] Both the number of carbon atoms in the chain and its odd or even nature are influential in determining the structure. The stable forms at low temperatures involve an orthorhombic crystal lattice in the case of odd numbers of carbon atoms. For even *n*-alkane chains with carbon numbers below 26, the structure is triclinic, whereas for 26 or more carbon atoms, it is monoclinic with an orthorhombic subcell. In addition, a rotator phase is formed at higher temperatures in many cases.

Following initial XRD studies on n-$C_{44}H_{90}$ by Müller,[2] the $Pca2_1$ orthorhombic structure was identified by Teare.[3] Sullivan and Weeks[4] obtained SAXS data for n-$C_{44}H_{90}$ crystallized from toluene solution as a function of temperature on heating to 356.5 °K and then on cooling down to room temperature. The long spacing was found to change with temperature and three crystal forms were identified: (011) monoclinic at lower temperatures, (101) monoclinic at higher temperatures, and orthorhombic I on cooling the (101) monoclinic form. The (011) monoclinic structure is the "normal" structure expected for an even paraffin, whereas increasing end group disorder with increasing temperature requires the transition to the (101) monoclinic structure in order to accommodate this. The enhanced disorder at higher temperatures leads, on cooling, to the orthorhombic I form, which can accommodate translationally disordered chains. Variable temperature ^{13}C NMR spectroscopy has also been used to identify an "intermediate phase" in $C_{44}H_{90}$ which occurs above 70 °C.[5] With the exception of the triclinic structure, all of the crystal forms quoted above have an orthorhombic subcell. In general, the stability of a particular phase is closely related to the packing of methyl end groups at the crystal surfaces, and in the present work we identify peaks in the infrared vibrational spectrum of tetratetracontane (n-$C_{44}H_{90}$) which characterize the environment of the methyl groups in the different crystal structures formed.

A new orthorhombic *Pbca* structure (later labelled "Orthorhombic II" by Kobayashi et al.[6]) was described by Boistelle et al. for n-$C_{28}H_{58}$ and n-$C_{36}H_{74}$ crystallized from light petroleum solutions.[7] A polytypic modification of the monoclinic structure, this form was described as a stacking of monoclinic layers, each successive one being the image of the previous layer through a rotation about a twofold axis perpendicular to the (001) plane. Within each layer, the alkane chains are inclined from the normal to the (001) plane at an angle of nearly 30°. More recently, high resolution synchrotron X-ray powder diffraction has been used to determine the unit cell parameters of n-$C_{44}H_{90}$ in the orthorhombic *Pbca* structure.[8] This structure is probably related to chains with low defect concentrations, allowing closer packing of the methyl end groups. The various crystal forms are shown schematically in Figure 1, together with shorthand notations which will be used here for the different structures. Note that the unit cell parameter c corresponds to two layers in the case of both the orthorhombic structures and the M_{101} form.

The use of infrared spectroscopy in the study of alkyl chain disorder was pioneered by Snyder, who identified localized CH_2 wagging vibrations arising from departures from the planar all-*trans* chain.[9] Bands at 1368 and 1308 cm^{-1} were assigned to conformational sequences *gtg* and *gtg′*, a band at 1352 cm^{-1} to the sequence *gg*, and one at 1344 cm^{-1} to the end-*gauche* conformation. These assignments have since been widely used to characterize the chain disorder in a range of systems,

* To whom correspondence should be addressed. E-mail: s.j.spells@shu.ac.uk. Phone: +44 (0) 114 225 3428. Fax: +44 (0) 114 225 3066.
† Sheffield Hallam University.
‡ Current address: Department of Engineering Materials, University of Sheffield, Sheffield S1 3JD, United Kingdom.
§ University of Sheffield.

10.1021/jp030794e CCC: $27.50
Published on Web 02/14/2004

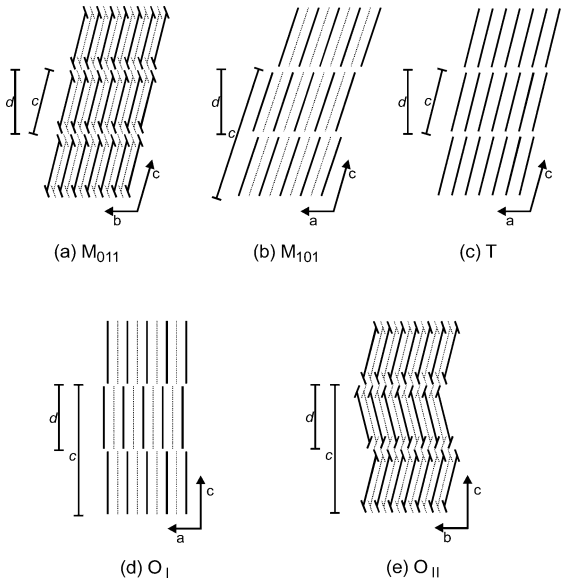

Figure 1. Schematic drawing of molecular packing in (a) monoclinic M_{011}, (b) monoclinic M_{101}, (c) triclinic T, (d) orthorhombic I (O_I), and (e) orthorhombic II (O_{II}) forms. The different packing modes of chain ends at the ordered layer surfaces of M_{011} and O_{II} phases are indicated by the end bars. The layer spacing d and the unit cell parameter c are also indicated.

including n-alkanes,[10] polyethylene,[11,12] long chain n-alkanes,[13,14] carboxylic acids,[15] phospholipids,[16] and surfactant molecules.[17] In many cases, the symmetric methyl deformation band at around 1378 cm^{-1} has been used as an internal reference band, to normalize data. In a wider spectroscopic study of a series of long chain n-alkane molecules, it became clear that such normalization was a critical procedure in the data analysis.[18] This led to the present investigation of n-$C_{44}H_{90}$, a shorter molecule incapable of chain folding, but nevertheless showing complex polymorphism.

In addition to the methylene wagging vibrations described above, various methyl vibrations also display conformational sensitivity, allowing the infrared spectrum to be used to characterize the end group environment. While the symmetric methyl ("umbrella") deformation is well known in the 1373−1378 cm^{-1} region for n-alkanes in the $Pca2_1$ orthorhombic crystal structure (e.g., ref 19), additional bands have been noted for other crystal forms: Nielsen and Holland, using polarized IR radiation and a reflecting microscope, assigned bands at 1368 and 1370 cm^{-1} to the symmetric methyl group deformation in the monoclinic forms of n-$C_{36}H_{74}$ and n-$C_{46}H_{94}$ respectively.[20] Bands at 1368 cm^{-1} (polarized in the direction of the b axis) and 1378 cm^{-1} (mainly polarized perpendicular to the ab plane) in the spectrum of monoclinic n-$C_{36}H_{74}$ were later assigned to the in- and out-of-phase components of the symmetrical deformation mode of adjacent methyl groups.[21] A single band at 1368 cm^{-1} in the triclinic form of n-$Cs_{18}H_{38}$, polarized parallel to the skeletal planes, was assigned to the symmetrical methyl deformation. The various crystal forms of n-$C_{36}H_{74}$ were investigated by Kobayashi et al.[6] In the normal (011) monoclinic form, bands at 1374 and 1372 cm^{-1} were identified, respectively, with the a and b polarized components of the symmetric methyl deformation. An orthorhombic II structure, with alternating layers as previously described by Boistelle et al.,[7] was identified from X-ray diffraction data and the splitting of the Raman-active longitudinal acoustic (LA) mode. It was characterized by IR bands at 1382 and 1370 cm^{-1} polarized in the a and b directions, respectively. A single band at 1376 cm^{-1} was observed for the usual "orthorhombic I" form. In summary, the symmetric methyl deformation has been observed in the region from 1368 to 1382 cm^{-1}, depending on crystal form, with differing polarizations.

The methyl C−H stretching region of the IR spectrum of n-alkanes has also been investigated, with temperature-dependent data for different crystal and clathrate forms related to the various mode assignments.[22,23] In particular, the positions of the in-phase and out-of-phase asymmetric stretch depend on the crystal structure and may themselves become doubled through factor group splitting. However, measurements have only been reported unambiguously for the triclinic and orthorhombic I structures (with doubling in the latter case) and for urea clathrates. Here, we extend the range of crystal structures characterized in this spectral region to include both monoclinic (011) and orthorhombic II forms.

The progression of rocking-twisting methylene vibrations in the region of the infrared spectrum from 700 to 1000 cm^{-1} has previously been studied.[10,19,24−27] The splittings were found to be dependent on the crystal structure. These bands are used in the present work to provide evidence of the relative chain disorder in different structures.

Finally, the band at around 890 cm^{-1} is ascribed to the methyl rocking mode and shows conformational sensitivity: Snyder[19] reported low temperature measurements showing a single band near 893 cm^{-1} for a triclinic crystal structure, a doublet at 889 and 893 cm^{-1} for a monoclinic structure, and a doublet at 891 and 894 cm^{-1} for an orthorhombic I structure.

Within the context of our ongoing study of long chain n-alkanes, and more generally in the use of the methylene wagging vibrations to characterize molecular disorder, it is important (i) to understand the restrictions involved in using the methyl symmetric deformation for spectral normalization and (ii) to make use of the sensitivity of the methyl group vibrations considered above to intermolecular interactions, enabling their use in characterizing the environments of the chain ends. In this respect, the work described here has wider relevance to a diverse range of functionalized n-alkanes, used in applications such as surface-passivated nanomaterials.[28] The present work, while providing spectroscopic characterization of the various crystal structures of n-$C_{44}H_{90}$, addresses point (i) above and involves the application of point (ii) to this material.

Experimental Section

Tetratetracontane (n-$C_{44}H_{90}$) was obtained from the Aldrich Chemical Company, with a quoted-purity of 99%. Samples were obtained by crystallization from solution in Aristar grade toluene and were prepared as follows:

(1) Sample crystallized from 1.3% w/v solution in toluene cooled to 25 °C, filtered and the resulting mat allowed to dry before pressing at less than 0.4 ton cm^{-2}.

(2) As sample 1, but pressed between 0.8 and 1.2 ton cm^{-2}.

(3) Sample crystallized from 0.45% w/v solution in toluene cooled to 25 °C, filtered and the mat allowed to dry without pressing.

(4) Sample crystallized from 0.27% w/v solution in toluene by cooling from 92 °C at 0.3 °C min^{-1}. The suspension was pipetted onto a KBr disk. After drying, a second KBr disk was used to cover the sample.

(5) A 0.33% w/v solution in toluene was pipetted onto a KBr disk at room temperature and allowed to crystallize. After drying, a second KBr disk was used to cover the sample.

Transmission infrared spectra were recorded at 1 cm^{-1} resolution, with typically 200 scans, using a Mattson 6021 FTIR spectrometer with a cooled narrow band MCT detector. Samples were held between KBr microscope windows fitted within a

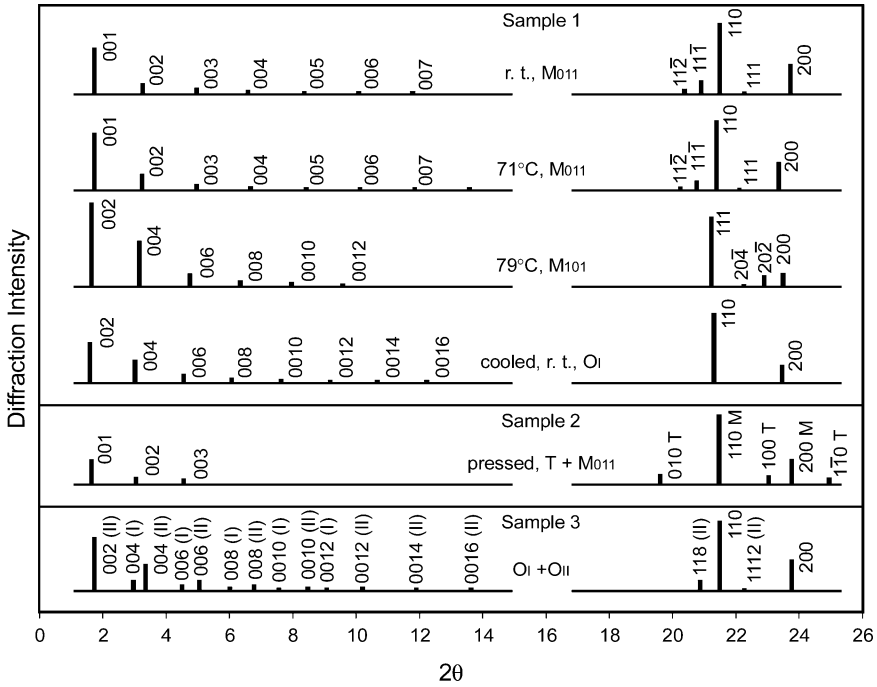

Figure 2. Diffractograms of $C_{44}H_{90}$ samples under various conditions. Diffraction intensities are normalized to the (110) diffraction for each diffractogram. The intensities of the low-angle peaks were multiplied by 3.

Graseby-Specac 20500 sample holder modified with steel inserts and PTFE collars to accept the windows. This was held inside a Graseby-Specac 21500 variable temperature cell linked to a 20120 temperature controller. Measurements were carried out within the range −173 to +90 °C, with a stability of ±1 °C. The sample holder was calibrated before use, with a miniature thermocouple at the sample position. Spectra are generally shown here after background subtraction.

We used a Mettler DSC 30 equipped with a low temperature cell and coupled to a Mettler-Toledo TA8000 thermal analysis system. 40 μL aluminum crucibles (ME-27331) were used. The heating rate used during the experiments was 2 °C min^{-1}.

Small and wide angle X-ray scattering (SAXS and WAXS) patterns from powder samples were recorded with an image plate area detector (MarResearch), using graphite-monochromatized Cu Kα radiation. Samples in capillaries were held in a custom-built temperature cell controlled to within 0.1 °C. The beampath up to the beamstop was flushed with helium gas.

Optical microscopy made use of an Olympus BH2 microscope with 100× objective.

Results

(1) X-ray Diffraction (XRD). Schematic XRD patterns for samples 1−3 are shown in Figure 2 and the corresponding layer *d*-spacings are listed in Table 1, together with theoretical values for different structures. There is generally good agreement between observed and calculated values. The structures found are summarized in Table 2 and spacings from wide angle diffraction are listed in Table 3.

(2) DSC. A DSC heating run on a sample initially in the M_{011} form is shown in Figure 3. An endotherm was observed at 75 °C, which is believed to be the temperature at which the phase transition between (011) and (101) monoclinic crystal forms occurs. A larger endotherm follows at 85 °C, corresponding to the melting temperature of the M_{101} crystal form. A phase transition was also observed from XRD measurements between 71 and 79 °C on sample 1. This transition is characterized by a change in the long spacing between the M_{011} form (long spacing 52.0 Å) and the M_{101} form (long spacing 55.0 Å) (Table 1, Figure 2).

TABLE 1: Experimental and Theoretical Layer *d*-Spacings of Various Forms of $C_{44}H_{90}$[a]

samples and conditions		layer spacings (Å) experimental	theoretical
sample 1	r.t., M_{011}	52	51.6
	71 °C, M_{011}	52	51.6
	79 °C, M_{101}	55	54.7
	cooled, r.t., O_I	57.5	57.9
sample 2	pressed, r.t., T	55	54.9
sample 3	O_I	58	57.9
	O_{II}	51.5	51.6

[a] Broadhurst's formulas[1] were used for theoretical calculations: $d_{OI} = 1.270 \times 44 + 1.98$, $d_{M011} = d_{OII} = 1.106 \times 44 + 2.93$, $d_T = 1.219 \times 44 + 1.28$, $d_{M101} = d_{OI} \cos(19°)$.

TABLE 2: Crystal Structures and Notations of Various Forms Found in $C_{44}H_{90}$[a]

sample		crystal system	layer surface	space group	notation
sample 1	r.t − 71 °C	monoclinic	$(011)_s$	$P2_1/b$[32]	M_{011}
	>79 °C	monoclinic	$(101)_s$	$A2^2$	M_{101}
	cooled, r.t.	orthorhombic	$(001)_s$	$Pca2_1$[3]	O_I
sample 2	pressed, r.t.	triclinic	$(001)_s$	$P\bar{1}$[30]	T
sample 3	r.t.	orthorhombic	$(001)_s$	$Pca2_1$	O_I
	r.t.	orthorhombic	$(011)_s$	$Pbca$[7]	O_{II}

[a] All structures, except the triclinic form,[30] adopt the same orthorhombic subcell of CH_2 groups.[31] Layer surfaces are represented by their corresponding crystal plane in the subcell lattice.

(3) FTIR. *(a) CH_2Wagging Region.* Figure 4 shows the wagging mode region of the IR spectrum for sample 1 as a function of temperature. Data are shown here, as in most cases, after baseline subtraction using Mattson software. Absorbance was set to zero at frequencies of 1400 cm^{-1} and 1260 cm^{-1}. As with all of the samples considered here, the full methylene wagging region of the IR spectrum (1390−1280 cm^{-1}) shows very low values of absorbance, indicating that stronger peaks observed here in the 1400−1360 cm^{-1} range are associated with

TABLE 3: Experimental Spacings of Wide Angle Diffractions[a]

	sample		spacings of diffraction peaks (Å)					cell parameters					
								a (Å)	*b* (Å)	*c* (Å)	α (°)	*β* (°)	*γ* (°)
1	r.t.	Index	$11\bar{2}$	$11\bar{1}$	110	111	200						
	M_{011}	exper.	4.34	4.24	4.12	3.98	3.74	7.48	5.53	58.4	117	90	90
		calc.	4.33	4.23	4.12	3.99	3.74						
	71 °C	Index	$11\bar{2}$	$11\bar{1}$	110	111	200						
	M_{011}	exper.	4.37	4.27	4.15	4.01	3.80	7.60	5.55	58.4	117	90	90
	calc.	4.36	4.27	4.15	4.02	3.80							
	79 °C	Index	111	$20\bar{4}$	$20\bar{2}$	200							
	M_{101}	exper.	4.17	3.96	3.87	3.77		8.02	4.99	116	90	109	90
	calc.	4.17	3.93	3.87	3.79								
	cool	Index	110	200									
	r.t.	exper.	4.16	3.78				7.56	4.98	115	90	90	90
	O_I	calc.	4.16	3.78									
2		Index	010	100	$1\bar{1}0$								
	T	exper.	4.51	3.85	3.56			4.27	4.77	58	90	108	108
		calc.	4.51	3.85	3.55								
		Index	110	200									
	M_{011}	exper.	4.12	3.73				7.46	5.55	/	117	90	90
		calc.	4.12	3.73									
3		Index	110	200									
	O_I	exper.	4.12	3.73				7.46	4.94	116	90	90	90
		calc.	4.12	3.73									
		Index	118	1110	1112	200							
	O_{II}	exper.	4.24	4.12	3.98	3.74		7.50	5.60	103	90	90	90
		calc.	4.24	4.11	3.98	3.75							

[a] The best fit cell parameters, index and calculated spacings are also included.

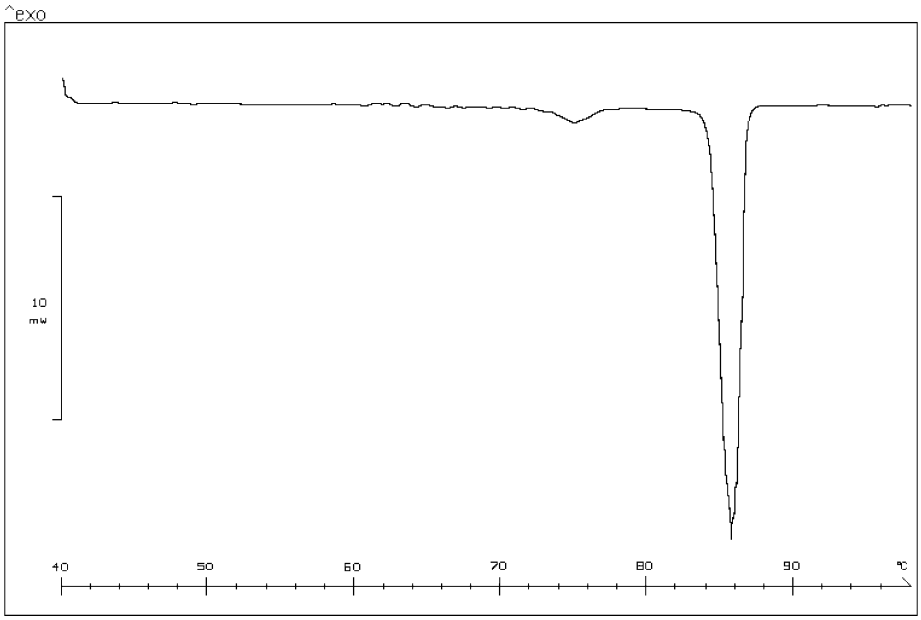

Figure 3. D.S.C. thermogram of sample 1. Heating rate 2 °C min^{-1}. The endotherm at 75 °C corresponds to the transition between M_{011} and M_{101} forms, with the latter form melting at 85 °C.

the methyl symmetric deformation. This is despite the fact that the 1371 cm^{-1} peak in Figure 4, for example, overlaps the expected CH_2 wagging mode from *gtg* and *gtg′* conformations at 1368 cm^{-1}. In fact, the near coincidence of these band frequencies led to their confusion in the literature, until the situation was resolved by Nielsen and Holland.[20] XRD measurements on the starting sample (sample 1) showed a long spacing of 52.0 Å, indicating an M_{011} structure, with a trace of O_I (57.5 Å layer spacing). The initial major IR peak at 1371 cm^{-1} is therefore ascribed to the symmetric methyl deformation of the M_{011} form, whereas the shoulder at 1377 cm^{-1} may arise from the orthorhombic structure. On the other hand, the assignment of both bands to a monoclinic structure would be consistent with the results of Holland and Nielsen.[21] However, their conclusion that the 1378 cm^{-1} band in n-$C_{36}H_{74}$ was mainly polarized perpendicular to the *ab* plane would suggest a low absorbance in a pressed mat, as used here. As noted above, the initial spectrum is dominated by the 1371 cm^{-1} peak, whereas wagging modes at 1302 and 1341 cm^{-1} have low absorbances. The implication is of highly regular chain conformations, with minimal numbers of gauche bonds.

On passing through the phase transition from M_{011} to M_{101} (confirmed by the XRD layer spacing of 55.0 Å; see Table 1), the methyl deformation is changed so that the peak at 1378 cm^{-1} now dominates. A significant increase in the absorbance of the end-*gauche* 1341 cm^{-1} peak is also observed, consistent with observations from ^{13}C NMR spectroscopy of n-$C_{44}H_{90}$, which have been interpreted as showing a noncrystalline state for the terminal carbon atoms on heating above 70 °C.[5] The use of second derivatives and spectral deconvolution, followed

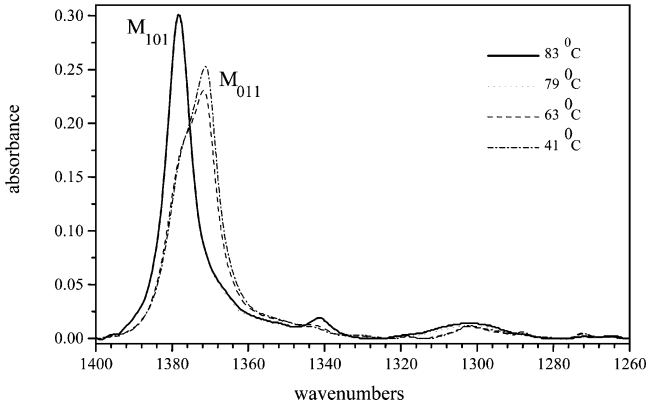

Figure 4. FTIR spectrum of sample 1 as a function of temperature, after baseline subtraction, showing the transition from M_{011} to M_{101} forms.

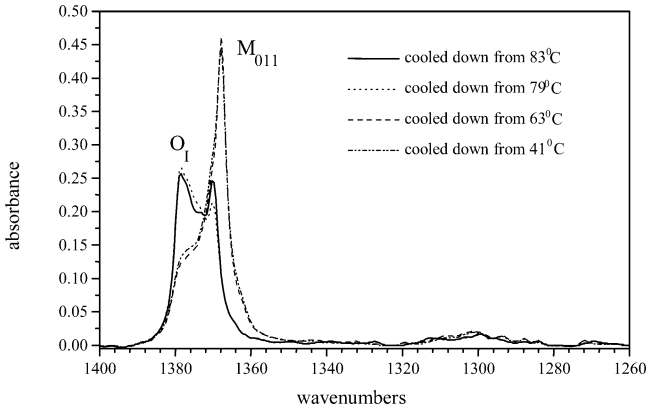

Figure 5. Low-temperature FTIR spectrum of sample 1 as a function of annealing temperature, showing the development of the O_I structure on cooling.

by curve fitting, indicated the presence of an additional band at 1365 cm^{-1}, with a temperature dependence closely resembling that of the 1371 cm^{-1} peak.

Room-temperature XRD data, after cooling this sample from 79 °C, show a spacing characteristic of the O_I form (57.5 Å) (Table 1). Low-temperature FTIR spectra in Figure 5 show enhanced peak separations. The sample as cooled from either 41 or 63 °C shows a peak at 1368 cm^{-1} together with shoulders at 1371 and 1379 cm^{-1}. The main band after conversion to the M_{101} phase is at 1379 cm^{-1}, with a second peak at 1370 cm^{-1} and an unresolved peak at 1374 cm^{-1}. In view of the XRD results, the peak at 1379 cm^{-1} should be attributed to the O_I phase formed on cooling. The strong 1368 cm^{-1} peak observed after cooling from lower annealing temperatures (41 and 63 °C) should probably be assigned to the M_{011} phase, which does not convert by cooling to the O_I form. In addition, a peak has been observed at approximately 1370 cm^{-1} in the FTIR spectrum of the extended chain form of n-$C_{198}H_{398}$,[18] which has the perpendicular orthorhombic structure. This suggests the assignment of the 1370 cm^{-1} peak obtained on cooling from 79 and 83 °C to the O_I form. However, we cannot rule out the possibility that the peak arises from residual unconverted M_{011} crystals.

The effect of applying higher pressure to the crystal mat is illustrated for sample 2 in Figure 6.

The initial spectrum shows bands at 1371 and 1377 cm^{-1}. WAXS measurements (Figure 2) showed the structure of the starting sample to be a mixture of M_{011} and triclinic forms. The IR peaks are, by comparison with data for sample 1 (Figure 4), assigned to M_{011} (1371 cm^{-1}) and triclinic (1377 cm^{-1}) forms.

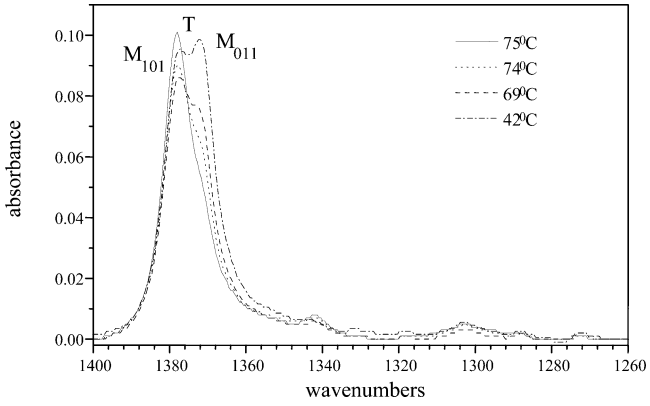

Figure 6. FTIR spectrum of sample 2 as a function of temperature. The transition from M_{011} to M_{101} structure is now partially obscured by the presence of the triclinic form.

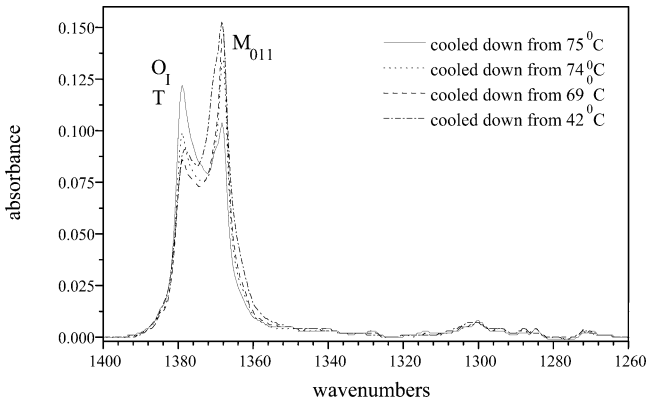

Figure 7. Low-temperature FTIR spectrum of sample 2 as a function of annealing temperature. Both triclinic and O_I forms are believed to contribute to the absorbance at 1379 cm^{-1}.

On increasing the temperature, Figure 6 shows a decrease in the intensity of the 1371 cm^{-1} band, followed by an increase in the 1378 cm^{-1} band intensity, consistent with conversion to the M_{101} phase and confirmed by XRD data. The 1341 cm^{-1} end-*gauche* band is evident in all spectra, with the absorbance increasing significantly at the phase transition. Low-temperature IR spectra of the wagging mode region are shown in Figure 7.

Although the general features of the spectra resemble those for sample 1 (Figure 5), it is possible to attribute the higher absorbance at 1379 cm^{-1} for samples cooled from 42 and 69 °C either to the additional presence of the triclinic form in this case or to a more complete conversion to the O_I form on cooling. This peak increases in absorbance once the sample has undergone the conversion to the M_{101} form, a factor which is again attributed primarily to the development of the O_I form on cooling.

Sample 3 was prepared in order to determine whether even lightly pressing the sample may influence the structure. Figure 8 shows the methylene wagging region at low temperatures for this unpressed sample. No baseline subtraction has been undertaken: the poor quality of the spectrum, with a significant and sloping background, is related to the absence of pressing and thus to enhanced scattering. Nevertheless, a new peak is evident at 1384 cm^{-1}. Following the assignment by Kobayashi et al. for n-$C_{36}H_{74}$,[6] we may associate this band with one of the symmetric stretching deformations of an O_{II} structure. The 1370 cm^{-1} band in Figure 8 can probably be attributed to a proportion of the M_{011} form or alternatively to the O_{II} phase. XRD measurements indicate the O_{II} form (or M_{011}, since these are not distinguishable) and, with smaller intensity, the O_I form.

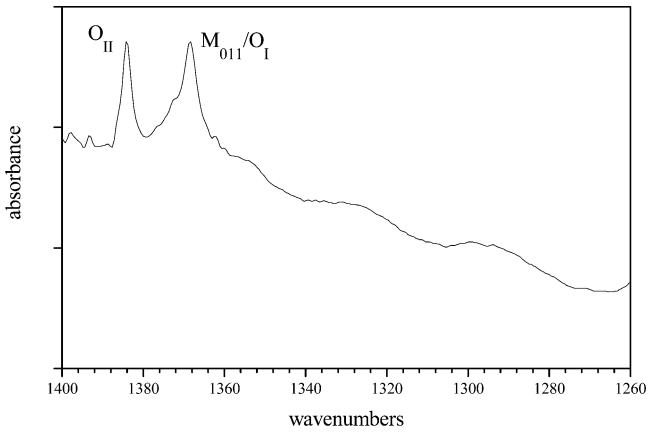

Figure 8. Low-temperature FTIR spectra for sample 3, which was not pressed. This accounts for the large sloping baseline. The 1384 cm^{-1} band is assigned to the O_{II} structure.

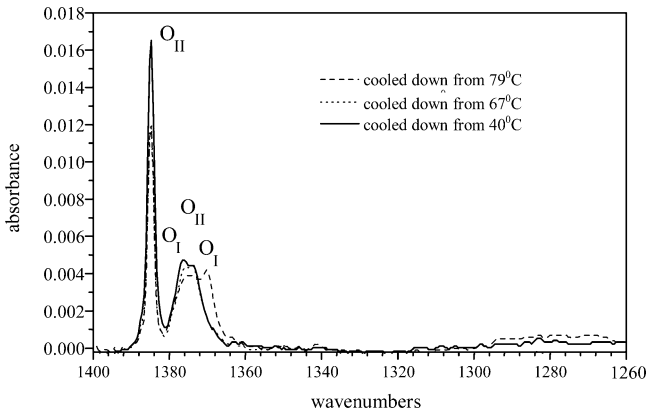

Figure 9. Low-temperature FTIR spectrum of sample 5 as a function of annealing temperature. The peak at 1373 cm^{-1} is tentatively assigned to the second component of the O_{II} symmetric methyl deformation. The O_{II} phase is clearly still present on cooling from 79 °C.

1384 cm^{-1} corresponds to the highest frequency observed for the methyl deformation, and this is consistent with very close packing of the methyl groups.

The preparation method for sample 4 produced a thin film suitable for optical microscopy, as well as for use of the IR-active methyl C−H stretching mode (see section 3c). Optical microscopy showed the large lozenges to be multi-layered. The IR spectrum in the 1400 to 1280 cm^{-1} region was similar to that of sample 1, indicating a structure which was predominantly M_{011} with some trace of O_I (respectively a strong peak at 1368 cm^{-1} and a small one at 1376 cm^{-1} at low temperatures). Transformation to the M_{101} form occurred on heating above 75 °C, and to the O_I form on cooling (1378 cm^{-1} peak at low temperature). Again, the 1370 cm^{-1} peak observed after cooling may relate to either or both of O_I and residual M_{011} forms. Sample 5 was also produced with the aim of forming a thin film. Optical microscopy revealed lozenge-shaped crystals, although these are likely to be multilayers. The IR spectrum in the wagging mode region showed the presence of a peak at 1384 cm^{-1} in the starting material, again indicative of the O_{II} structure. The peak absorbance was reduced on heating, with a simultaneous increase in absorbance of the band at 1377 cm^{-1}, suggesting the presence of some O_I crystals.

Corresponding low temperature spectra in Figure 9 show the 1384 cm^{-1} band to be predominant, whereas this was not the case for sample 3 (Figure 8). Our interpretation is that sample 5 initially has the larger proportion of the orthorhombic II phase. For this reason, we tentatively associate the 1373 cm^{-1} peak at

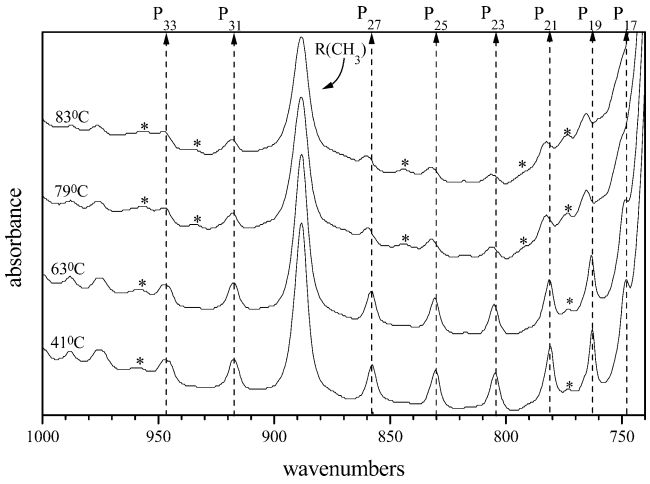

Figure 10. Methylene rocking-twisting mode region of the infrared spectrum of sample 1 as a function of the temperature. Even order progression bands (∗) are more apparent at the higher annealing temperatures, where the predominant crystal form is M_{101}, rather than M_{011}.

the lower temperatures with the second component of the symmetric methyl deformation in the O_{II} structure. The third band at around 1376 cm^{-1} is believed to be due to crystals of the O_I form. Spectra recorded at the annealing temperature indicate a decrease in the 1384 cm^{-1} absorbance with increasing temperature: it might be supposed that this indicates a phase transition, but Figure 9 shows that the 1384 cm^{-1} peak persists on cooling after annealing at higher temperatures. It is possible that this observation is a consequence of a change in the orientation of the chain axis occurring in the O_{II} crystal structure relative to the sample normal. The appearance of a peak at 1370 cm^{-1} after heating to 79 °C (Figure 9) together with the broad band around 1376 cm^{-1} indicates the presence of the O_I form.

The predominantly reversible nature of the spectral changes in the wagging region suggests that the chain ends become rapidly disordered on heating above room temperature. The apparent absence of any significant increase in the proportion of end-*gauche* conformations with heating should not be taken as a definitive conclusion, since the signal-to-noise ratio is poor in this region. There is then the question of stacking faults within the O_{II} crystal structure. A single alternation of tilt angle in successive layers within the O_{II} crystal structure is presumably a prerequisite for observing the methyl deformation component at 1384 cm^{-1} and the splitting of the Raman LA mode,[33] whereas some regularity of alternation is necessary to observe the characteristic X-ray periodicity. It does not necessarily follow that *all* crystals are in the O_{II} form, rather than the M_{011} structure, although in this case the large 1384 cm^{-1} absorbance indicates that the O_{II} structure initially predominates.

(b) CH_2 Rocking Region. The methylene rocking mode region of the higher temperature spectra of sample 1 is shown in Figure 10 (spectra have been translated upward for a more convenient presentation). Each one of the progression bands present in this region (crossed by a vertical dashed line) is ascribed to a non-localized mode involving the motion of adjacent methylene groups with the same phase difference along the *n*-alkane chain. This phase difference is proportional to an integer k and can be used to identify each one of these progression bands. For an *n*-alkane chain in an all-*trans* conformation, only the odd members of the progression bands (k odd) are infrared active.[19,24] In Figure 10, the infrared bands crossed by a vertical dashed line are assigned to the odd progression bands and labelled by P_k.[10] The most intense band at around 888 cm^{-1} is ascribed to

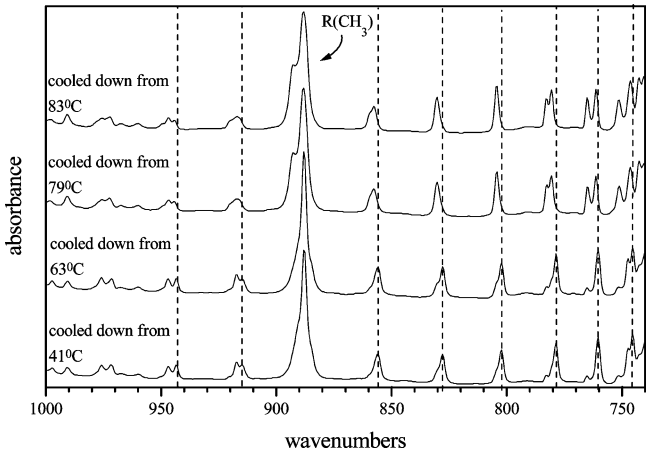

Figure 11. Low-temperature spectrum of sample 1 recorded in the methylene rocking−twisting mode region. Note the absence of even order progression bands, indicating ordered structures, and the presence of band splittings, particularly after annealing at higher temperatures.

the methyl symmetric rocking mode. Unfortunately, due to the number of carbon atoms involved in the *n*-$C_{44}H_{90}$ extended chains, the 29th member of the band progression is believed to be covered by this last band. Those marked with an asterisk are believed to be the even progression bands, which are only active in the infrared spectrum if the *n*-alkane chains contain at least one gauche conformer. Up to 63 °C, only small changes in the odd bands are observed. The alkane chains are expected to be essentially in the all-*trans* conformation, although the presence of one even band at around 772 cm^{-1} indicates the presence of at least some gauche conformers in the chains. Above this temperature, a shift of the odd bands toward higher wavenumbers occurs with a clear decrease in their intensity. This shift in frequency may be related to the more disordered M_{101} form, with a shorter all-*trans* chain length. New even progression bands, marked by an asterisk, are developing between the original odd progression bands. In particular, the localized band at around 955 cm^{-1} is assigned to specific end-*gauche* conformers.[10] The even progression bands indicate an increase of gauche conformers, preferentially near the ends of the chains. This conclusion is based on the fact that the chain length-dependent band frequencies are not significantly changed. This is also in accord with measurements of the gauche bond distribution along the chain for *n*-$C_{21}H_{44}$.[34] A significant disordering of chains, near to their ends, is thus observed above the transition temperature (75 °C).

The same region of the low temperature spectra is shown in Figure 11. In these spectra recorded at −173 °C, only the odd members of the progression bands are present: at −173 °C, the *n*-alkane chains are in a highly ordered extended form, whatever the crystal structure. Also, at this low temperature, splitting of the progression bands can be observed. The relative intensity of the components differs from one band to another. Going from the M_{011} phase to the O_I phase, the higher frequency component increases in absorbance relative to the lower frequency component for each progression band. The positions of these maxima could be used, in principle, to identify the crystal structure for this *n*-alkane sample. Also, it should be noted that in some cases more than two components can be observed.

Within the methylene rocking mode region of the infrared spectra shown in Figure 12, a band at around 888 cm^{-1} is ascribed to the methyl rocking mode. Although a strong band appears at 888 cm^{-1} in all spectra, the 891 cm^{-1} shoulder in samples which have been cooled from 41 and 63 °C is replaced

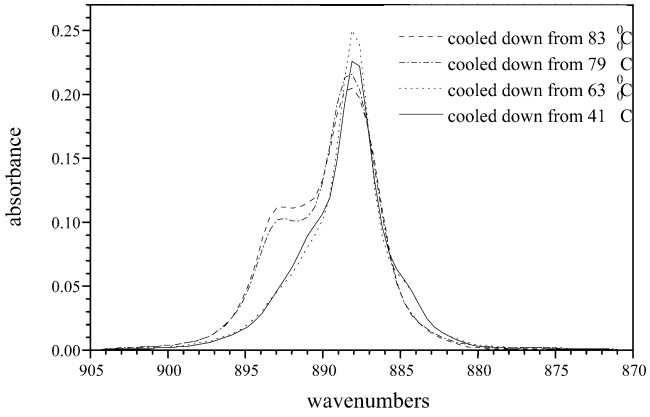

Figure 12. Methyl rocking region of the low temperature FTIR spectrum of sample 1 as a function of annealing temperature, showing the development of the O_I structure on cooling.

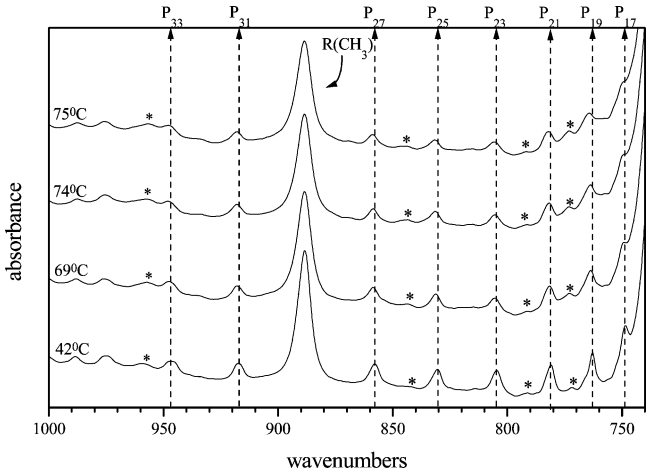

Figure 13. Methylene rocking-twisting mode region of the infrared spectrum of sample 2 as a function of the temperature. Even order progression bands (∗) are evident in all spectra, indicating disordered structures at all temperatures.

by a band at 893 cm^{-1} in the samples cooled from 79 and 83 °C. It has already been noted that the splitting of this band has been reported to be larger for a monoclinic crystal structure than for the O_I form.[19] Nevertheless, in view of the X-ray diffraction results quoted here, both the 888 and 893 cm^{-1} peaks can probably be attributed, at least in part, to the O_I form, although some contribution, at least to the 888 cm^{-1} peak, from the M_{011} form is likely. The 891 cm^{-1} shoulder may also relate to the M_{011} form.

The methylene rocking mode region of the high-temperature spectra for sample 2 is shown in Figure 13. The bands marked with an asterisk, ascribed to non all-*trans* chain conformations, are observed in the spectrum recorded at 42 °C. These indicate the presence of gauche conformers, most probably positioned at the end of the chains. With increasing annealing temperature, an increase in the intensity of the bands assigned to the gauche conformers is observed. At the same time, a decrease in peak height and a broadening of the odd bands occur. Nevertheless, no clear shift in the position of the odd bands is detected. The phase transition to the M_{101} form may have been partially completed at the higher temperatures. By comparison with sample 1 (Figure 11), more disorder is present at the lowest temperatures, on the evidence of the increased absorbance of the even order bands. This is a direct consequence of the increased pressure applied to this sample.

Low-temperature spectra, recorded at −173 °C, showed only the odd members of the progression bands to be present. At

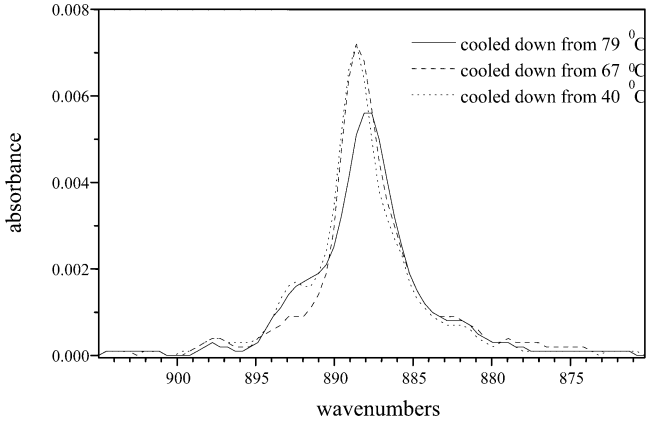

Figure 14. Methyl rocking region of the low temperature FTIR spectrum of sample 5 as a function of annealing temperature. The frequency shift in the main peak is attributed to partial conversion of the O_{II} form, possibly to the O_I form.

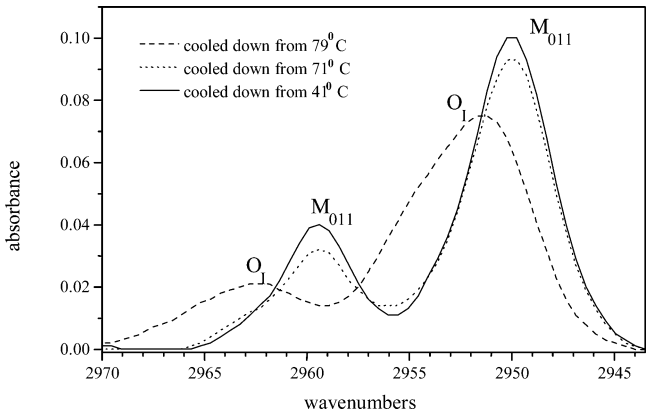

Figure 15. Low-temperature methyl C−H stretching region of the FTIR spectrum of sample 4. Transformation from the M_{101} to the O_I structure on cooling from 79 °C results in a frequency shift in both bands.

−173 °C, the *n*-alkane chains are in a highly ordered extended form, whatever the crystal structure. The relative intensities of the band components differed from one band to another. However, for each band, the different components were still present in the spectrum of the sample after annealing up to 75 °C. This strongly suggests that a mixture of phases is still present, as was observed in Figure 11. The band profiles in the methyl rocking region were found to be similar to those of sample 1, making it difficult to attribute any feature unambiguously to the initial triclinic form.

Figure 14 shows the methyl rocking mode region of the IR spectrum of sample 5. The major peak, initially at 889 cm^{-1}, is taken to be characteristic of the O_{II} form. This peak shifts toward 888 cm^{-1} for the final sample. Reproducibility of the smaller peak at 893 cm^{-1} is poor, with such a low absorbance.

(c) Methyl C−H Stretching Region. Figure 15 shows part of the methyl C−H stretching region of the low temperature spectrum of sample 4. The M_{011} structure is newly characterized here by asymmetric stretching bands (r_a^- and r_b^- in the nomenclature of MacPhail et al.[22]) at 2959 and 2950 cm^{-1}. The transition to the predominantly orthorhombic I phase results in peak shifts to 2962 and 2951 cm^{-1} and also in the broadening of both peaks to higher frequencies, consistent with previous data.[22] The broadening probably indicates a splitting, not completely resolved at this temperature, of each peak into a doublet, as a result of intermolecular coupling.[23] The same region for sample 5 is shown in Figure 16. Further characterization of the O_{II} structure is now possible, with peaks at 2962 and 2951 cm^{-1}. Although these positions are identical to those assigned to the O_I phase in sample 4 after conversion to the M_{101} phase and cooling, the bands are initially narrower. After the final annealing at 79 °C, shoulders have appeared at around 2955 and 2967 cm^{-1}, whereas the former peaks show a decrease in absorbance. The shoulders seem to relate to the broadening, as observed for sample 4 on conversion to the O_I structure. Both the splittings of the r^- asymmetric stretching bands (approximately 11 cm^{-1}) and the splittings of the band components in the O_I structure (approximately 4−5 cm^{-1}) are of similar magnitude to figures quoted for n-$C_{20}H_{42}$ and n-$C_{21}H_{44}$ at similar temperatures.[23]

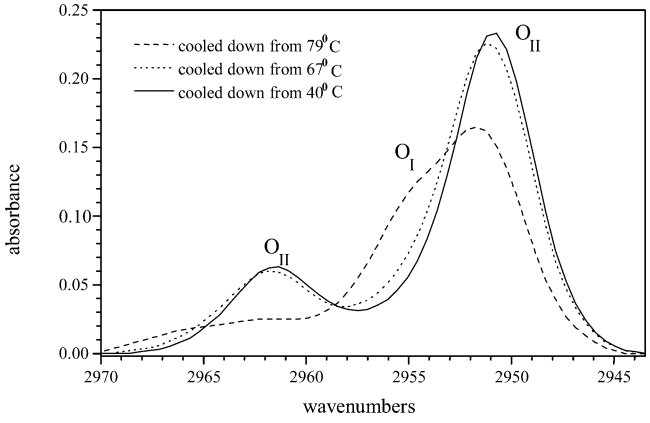

Figure 16. Low-temperature methyl C−H stretching region of the FTIR spectrum of sample 5. After heating to 79 °C, the appearance of shoulders is attributed to the O_I structure.

Discussion

Table 4 summarizes the frequencies of methyl group IR vibrations observed for n-$C_{44}H_{90}$. The symmetric deformation shows considerable complexity, and the components are probably not restricted to those quoted here: we list only those which can be identified with some degree of confidence. The results help to explain previous observations of various methyl symmetric deformation frequencies, including several references to peaks around 1384/5 cm^{-1} for different *n*-alkanes (e.g., ref 19). Table 4 provides new assignments for M_{011} and O_{II} structures, besides including additional detail of band positions in structures which have previously been studied.

Although the methyl group peak positions may be helpful in identifying crystal structures in n-$C_{44}H_{90}$ and other *n*-alkanes, it should be noted that the results depend on the specific forms of methyl group interactions. They are critically dependent on the nature of the crystal surfaces, rather than the structure of the crystal interior. One feature of this dependence is shown in the IR data collected above 75 °C. Here, the peak frequency in the methyl symmetric deformation region invariably tends to around 1378 cm^{-1}. In view of the other indications of increasing disorder, such as the increased intensity of the end-*gauche* CH_2 wagging mode and the even order CH_2 rocking progression bands, it would appear that the frequency of 1378 cm^{-1} is characteristic of a highly disordered crystal surface. Indeed, the frequency corresponds to that observed in the liquid state for many materials. At the same time, it is probably unreasonable to associate this band with any specific crystal form. The results may, nevertheless, have general significance beyond those crystal structures considered here. Indeed, the methyl group vibrations provide a conformational probe in addition to the methylene wagging region.

TABLE 4: Characteristic Frequencies of Methyl Group Vibrations and the End-*gauche* Methylene Wagging Vibration in Different Crystal Forms of Tetratetracontane

phase	methylene wagging (end-*gauche*)/cm^{-1}	methyl symmetric deformation/cm^{-1}	methyl rocking[a]/cm^{-1}	methyl C−H stretching[a]/cm^{-1}
monoclinic (011)		1371 1368−1370[a]	888? 891?	2950 2959
monoclinic (101)	1341	1378[b]		
triclinic	1341	1377 1379?[a]		
orthorhombic I	−[a]	1377 1370,[a] 1376−1379[a]	888 893	2951 2962 + shoulders at 2955 and 2957
orthorhombic II	−	1384 1384[a] 1373?[a]	889	2951 2962

[a] Measurements at −173 °C. [b] Denotes a band which is probably not specific to this crystal form.

There are several implications from this work for the use of methylene wagging mode vibrations in general. First, the frequency range of the symmetric methyl deformation is seen from Table 4 to extend from 1368 to 1385 cm^{-1}. This range significantly overlaps the 1368 cm^{-1} methylene wagging vibration from *gtg* and *gtg′* conformations. In the structures studied here, the methylene wagging vibrations generally show negligible absorbance, so the assignment of peaks in the range 1368 to 1385 cm^{-1} to methyl group vibrations is unambiguous. In principle, for systems with greater disorder, it is important to be aware of the possibility of overlapping bands in estimating the proportion of *gtg/gtg′* conformations from the 1368 cm^{-1} band area. Second, the methodology of using methylene wagging bands for quantitative estimates of the chain disorder requires some reconsideration. Much previous work (e.g., refs 16 and 35) has made use of the 1378 cm^{-1} symmetric methyl deformation for spectral normalization. Clearly the presence of other crystal structures listed in Table 1 will result in additional peaks in this region of the spectrum. Phase transitions between crystal forms are, on the basis of this work, likely to change the characteristics of the symmetric methyl group deformation and lead to erroneous quantitative estimates of the disorder present. The methyl rocking vibration has also been used for the normalization of IR intensities (e.g., ref 36). The presence of a member of the methylene rocking progression bands may result in additional peaks in the neighborhood of the methyl rocking band. Indeed, taking the example of the infrared spectrum of *n*-$C_{44}H_{90}$, the 29th member of the progression bands is overlapped by the more intense band at 888 cm^{-1} assigned to the methyl rocking mode. Hence, the use of this last band for spectral normalization could, once again, lead to erroneous quantitative estimates of the disorder present.

Third, the different polarizations of the symmetric deformation modes for the different crystal structures of *n*-alkanes, noted in the Introduction, imply that changes in molecular orientation can modify the relative absorbances of these modes. Again, this has practical significance for the normalization of methylene wagging vibrations.

It should be noted here that the presence of "chain tilt", in the form of monoclinic crystal structures, has a different origin from the continuous variation in tilt angle recently studied in long chain *n*-alkanes.[37] In the present case, the (011) monoclinic form is related to the even number of carbon atoms, whereas the transformation to the (101) monoclinic form results from increased chain end disorder and packing considerations at the crystal surface. In the case of long chain *n*-alkanes, successive annealing and cooling steps lead to a "perfecting" of the chain ends and the chains tilt to accommodate this. The tilt angle increases continuously up to around 35 °C, and there is a close parallel in the behavior of semicrystalline polyethylene.[38]

Conclusions

On crystallization of *n*-$C_{44}H_{90}$ from toluene solutions, the crystal structures (011) monoclinic, orthorhombic I, and orthorhombic II have been identified, on the basis of FTIR and X-ray diffraction measurements. An IR peak at 1384/5 cm^{-1} was assigned to the orthorhombic II structure on the basis of the attribution of a doublet at 1382 and 1370 cm^{-1} in the spectrum of *n*-$C_{36}H_{74}$ to the symmetric methyl deformation of this form.[6] We tentatively assign a peak at 1373 cm^{-1} to the second doublet component in *n*-$C_{44}H_{90}$. It was found to be difficult to prevent transformation of the crystal structure to the (011) tilted monoclinic form: indeed, Kobayashi et al. commented that "uncontrollable slight differences in crystallization conditions" could give rise to the two structures in *n*-$C_{36}H_{74}$.[6] Deliberate application of pressure tended to produce a proportion of triclinic structure. A phase transition from the (011) monoclinic to the (101) monoclinic form was identified at 75 °C.

The characteristic frequencies of the CH_3 symmetric deformation are listed in Table 4, indicating significant differences with crystal structure. Differences in the methyl group environment are also reflected in the CH_3 rocking and C−H stretching frequencies in Table 4. The only structures showing chain end disorder on the basis of the 1341 cm^{-1} end-*gauche* methylene wagging band were the (101) tilted monoclinic form and the triclinic structure, and significant intensity was only observed for elevated temperatures. The presence of even order bands in the methylene rocking progression also indicates a higher degree of chain disorder in these structures than for the (011) monoclinic and orthorhombic I structures.

The results presented in this work provide a basis for the use of IR spectroscopy to probe chain end disorder and packing, together with crystal structure, in a diverse range of applications.

Supporting Information Available: Further IR spectra of sample 2 (methylene rocking-twisting and methyl rocking regions at low temperatures, following annealing) and sample 5 (wagging mode region as a function of annealing temperature). This material is available free of charge via the Internet at http://pubs.acs.org.

References and Notes

(1) Broadhurst, M. G. *J. Res. Natl. Bur. Stand.* **1962**, *A66*, 241.
(2) Müller, A. *Proc. R. Soc. A* **1932**, *138*, 514.
(3) Teare, P. W. *Acta Crystallogr.* **1959**, *12*, 294.
(4) Sullivan, P. K.; Weeks, J. J. *J. Res. Natl. Bur. Stand.* **1970**, *A74*, 203.

(5) Ishikawa, S.; Kurosu, H.; Ando, I. *J. Mol. Structure* **1991**, *248*, 361.
(6) Kobayashi, M.; Kobayashi, T.; Itoh, Y.; Chatani, Y.; Tadokoro, H. *J. Chem. Phys.* **1980**, *72*, 2024.
(7) Boistelle, R.; Simon, B.; Pepe, G. *Acta Crystallogr.* **1976**, *B32*, 1240.
(8) Craig, S. R.; Hastie, G. P.; Roberts, K. J.; Sherwood, J. N. *J. Mater. Chem.* **1994**, *4*, 977.
(9) Snyder, R. G. *J. Chem. Phys.* **1967**, *47*, 1316.
(10) Maroncelli, M.; Qi, S. P.; Strauss, H. L.; Snyder, R. G. *J. Am. Chem. Soc.* **1982**, *104*, 6237.
(11) Painter, P. C.; Havens, J.; Hart, W. W.; Koenig, J. L. *J. Polym. Sci.* **1977**, *15*, 1223.
(12) Spells, S. J.; Organ, S. J.; Keller, A.; Zerbi, G. *Polymer* **1987**, *28*, 697.
(13) Ungar, G.; Organ, S. J. *Polym. Commun.* **1987**, *28*, 232.
(14) Gorce, J.-P.; Spells, S. J. *Polymer* **2002**, *43*, 2581.
(15) Zerbi, G.; Conti, G.; Minoni, G.; Pison, S.; Bigotto, A. *J. Phys. Chem.* **1987**, *91*, 2386.
(16) Senak, L.; Davies, M. A.; Mendelsohn, R. *J. Phys. Chem.* **1991**, *95*, 2565.
(17) Barron, C.; Spells, S. J. *J. Phys. Chem.* **1993**, *97*, 6737.
(18) Gorce, J.-P.; Spells, S. J. *Polymer*, submitted.
(19) Snyder, R. G. *J. Mol. Spectrosc.* **1960**, *4*, 411.
(20) Nielsen, J. R.; Holland, R. F. *J. Mol. Spectrosc.* **1960**, *4*, 488.
(21) Holland, R. F.; Nielsen, J. R. *J. Mol. Spectrosc.* **1962**, *8*, 383.
(22) MacPhail, R. A.; Strauss, H. L.; Snyder, R. G.; Elliger, C. A. *J. Phys. Chem.* **1984**, *88*, 334.
(23) MacPhail, R. A.; Snyder, R. G.; Strauss, H. L. *J. Chem. Phys.* **1982**, *77*, 1118.
(24) Snyder, R. G. *J. Mol. Spectrosc.* **1961**, *7*, 116.
(25) Snyder, R. G.; Schachtschneider, J. H. *Spectrochim. Acta* **1963**, *19*, 85.
(26) Snyder, R. G.; Maroncelli, M.; Qi, S. P.; Strauss, H. L. *Science* **1981**, *214*, 188.
(27) Snyder, R. G. *J. Chem. Phys.* **1979**, *71*, 6391.
(28) Meulenberg, R. W.; Strouse, G. F. *J. Phys. Chem. B* **2001**, *105*, 7438.
(29) Pieczek, W.; Strobl, G. R.; Malzahn, K. *Acta Crystallogr. B* **1974**, *30*, 1278.
(30) Mnyukh, Yu. V. *J. Struct. Chem.* **1960**, *1*, 370.
(31) Bunn, C. W. *Trans. Faraday Soc.* **1939**, *35*, 482.
(32) Shearer, H. W.; Vand, V. *Acta Crystallogr.* **1956**, *9*, 379.
(33) Kobayashi, M.; Sakagami, K.; Tadokoro, H. *J. Chem. Phys.* **1983**, *78*, 6391.
(34) Snyder, R. G.; Maroncelli, M.; Strauss, H. L.; Elliger, C. A.; Cameron, D. G.; Casal, H. L.; Mantsch, H. H. *J. Am. Chem. Soc.* **1983**, *105*, 133.
(35) Almirante, C.; Minoni, G.; Zerbi, G. *J. Phys. Chem.* **1986**, *90*, 852.
(36) Kim, Y.; Strauss, H. L.; Snyder, R. G. *J. Phys. Chem.* **1989**, *93*, 7520.
(37) de Silva, D. S. M.; Zeng, X. B.; Ungar, G.; Spells, S. J. *Macromolecules* **2002**, *35*, 7730.
(38) Bassett, D. C.; Frank, F. C.; Keller, A. *Phil. Magn.* **1963**, *8*, 1753. Bassett, D. C.; Hodge, A. M. *Proc. R. Soc. London A* **1981**, *377*, 25.